Energy 270 (2023) 126829

Contents lists available at ScienceDirect

Energy

journal homepage: www.elsevier.com/locate/energy

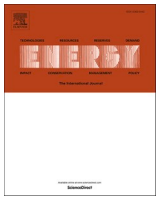

The impact of battery operating management strategies on life cycle cost assessment in real power market for a grid-connected residential battery application

Masoume Shabani [a,*], Fredrik Wallin [a], Erik Dahlquist [a], Jinyue Yan [a,b]

[a] School of Business, Society & Engineering, Department of Sustainable Energy Systems, Mälardalen University, Sweden
[b] Department of Building Environment and Energy Engineering, Hong Kong Polytechnic University, Hong Kong

ARTICLE INFO

Keywords:
Stationary battery storage
Calendric and cyclic ageing
Battery SOC control strategies
Battery lifetime improvement
Arbitrage application
Life cycle cost assessments under real power market

ABSTRACT

The relatively short lifetime of batteries is one of the crucial factors that affects its economic viability in current electricity markets. Thus, to make batteries a more viable technology in real power market from life cycle cost assessment perspective, full understanding of battery ageing parameters and which operating control strategies cause slower degradation rate is essential and still an open problem. This study deals with the 32 different battery operating control strategies to evaluate their importance on cyclic and calendric degradation, lifetime, and life cycle cost assessment of a battery system in a grid-connected residential application. In other words, it is evaluated that at which operating control strategy the system simulation results in a more beneficial system from techno-economic perspective. A battery modelling scenario is proposed to accurately estimate battery performance, degradation, and lifetime under real operational condition given different operating control strategies. An operational strategy, which benefits from the dynamic real-time electricity price scheme, is conducted to simulate the system operation. The key results show that selecting a proper state-of-charge control strategy positively affects the battery lifetime and consequently its net-present-value, in which the best strategy led to 30% improvement in net-present-value compared to the worst strategy.

1. Introduction

Battery storage system has emerged as the promising technology in providing several services in stationary applications in residential, commercial, and industrial sectors [1,2].The services can generally be classified into the end-user energy management services such as power quality and reliability, services for renewable energy applications such as renewable time-shifting and renewable firming, ancillary services such as load following, and frequency regulation, and bulk energy services such as energy arbitrage and peak shaving [3–6]. According to International Energy Agency [7], excluding pumped hydro storage, more than 90% of the new energy storage installations in stationary applications are driven by lithium-ion (Li-ion) batteries which has become an optimistic storage technology due to the features such as high round-trip efficiency, long cyclability, low operation, and maintenance cost, and flexibility for charging and discharging [8–10]. The prices of Li-ion batteries for stationary applications have fallen by almost two-third since 2010, due to the technical development in battery chemistries and innovative manufacturing processes. Further balance of system cost reduction and approachability of second-life batteries would lead to battery storages being 70% cheaper than today by 2040, which make the battery storage a dominant and viable storage technology by 2040 [7]. Moreover, electricity market is undergoing the rapid changes and volatile behavior, hence, participating the batteries in arbitrage market and exploiting the highly variable behavior of electricity prices can lead to revenue for both residential and commercial sectors. The idea behind the electricity price arbitrage strategy is to benefit from the daily electricity price differential through storing electricity during off-peak hours and using the stored electricity during peak hours [11–13]. Exploiting the price arbitrage, not only reduces the load on the grid during peak hours, but the customer electricity consumption can be managed in a more flexible and cost-effective way [14]. Moreover, shifting the energy consumption from on-peak to off-peak hours lead to the customer electricity bill reduction [15]. However, there are still challenges about the economic viability of battery storage in electricity markets. One of the crucial factors that affects battery economic profitability in real-life applications is its lifetime and capacity degradation

* Corresponding author.
E-mail address: masoume.shabani@mdu.se (M. Shabani).

https://doi.org/10.1016/j.energy.2023.126829
Received 18 September 2022; Received in revised form 23 January 2023; Accepted 27 January 2023
Available online 7 February 2023

Nomenclature

Abbreviations

AIP	Ageing influence parameter
BOL	Beginning of life
DOC	Depth of cycle of a battery
EOL	End of life
FEC	Full equivalent cycle of a battery
Grp	Group
$ICC_{battery}$	Initial investment cost of a battery
$LCC_{battery}$	Life cycle cost of a battery
LF	Battery lifetime
LCCA	Life cycle cost assessment
LFP/C	Lithium-iron phosphate ($LiFePO_4$/C)
NPV	Net present value
OCV	Open circuit voltage
RTP	Real-time price
$SSR_{battery}$	Self-sufficiency ratio
SOC	Battery state of charge
SOC op. window	Battery allowable SOC operation window
SOH	Battery state of health
SW	Controllable switches
TMS	Thermal management system

Symbols

$C_{O\&M}$	Maintenance and operation cost
C_{batt}	Battery capacity
C_{fade,cal_i}	Calendric capacity fade at time i (%)
C_{fade,cyc_i}	Cyclic capacity fade at time i (%)
C_{fade,tot_i}	Total capacity fade at time i (%)
d	Charge/discharge duration (h)
$I_{ch(dch),\ i}$	Battery charge (discharge) current at time i
$El_{w,i}$	Wholesale electricity price at time i
$El_{r,i}$	Retail electricity price at time i
n	n-th year of the project
MA_{RTP_m}	Moving average of RTP at time i of day m
$P_{batt,i}$	Battery power at time i
$P^{ch}_{min,i}$	Maximal charge power at time i
$P^{dch}_{max,i}$	Maximal discharge power at time i
$P_{batt-load,i}$	Transferred power from the battery to the load at time i
$P_{batt-grid,i}$	Exported power from the battery to the grid at time i
$P_{grid-batt,i}$	Imported power from the grid to the battery at time i
$P_{grid-load,i}$	Imported power from the grid to the load at time i
r	r-th replacement
R	Total number of replacements during the project lifetime
$R_{ch(dch),\ i}$	Battery internal resistance at time i
T	Temperature (K)
$time$	Passed time since the BOL (Sec)
$t_{ch,start,m}$	Start time indicator for charging the battery at day m
$t_{dch,start,m}$	Start time indicator for discharging the battery at day m
$V_{ch(dch),\ i}$	Battery terminal voltage during charging (discharging) at time i

Greek Symbols

$\delta_{Replace}$	Battery replacement indicator

[16–18]. The understanding of battery degradation mechanism and the impact of battery ageing is important from both research perspectives of '' battery cell design and manufacturing'' and battery management in application'' and should be considered to properly optimize battery design and battery management [19]. The battery ageing can be postponed through different measures such as (a) methods which are implemented during battery cell manufacturing processes; and (b) methods which can be applied as the battery operating control strategies for proper and efficient use of batteries in an application, which the latter is the aim of this study. From cell design perspective, one of the effective methods for improving battery cycle life and cell cyclability is to add additives to electrolyte of Li-ion batteries [20–22]. There are a number of electrolyte additives available for the Li-ion batteries which are able to improve the properties of Li-ion cells and can be divided into different categories [23] such as (1) solid electrolyte interface (SEI) layer improver, (2) Li deposition improver, (3) cathode protection agent, (4) safety protection agent, (5) LiPF6 salt stabilizer, (6) other agents such as solvation enhancer, Al corrosion inhibitor, and wetting agent. However, the aforementioned method can be applied in the manufacturing processes of Li-ion battery cell and is out of scope of current study which focuses on battery life improvement from battery management perspective. In other words, the current study explores strategies to address how to use the "purchased battery'' in the real-life application in a feasible and economic way in order to slower battery degradation rate and increase the value of battery in the application. Even with the development in battery chemistry and innovative manufacturing processes for improvement of battery cycle life such as adding different electrolyte additives, adopting proper battery operation control strategies can play key role and is necessity for prolonging battery life longevity to make batteries more viable technology in current and future electricity market. The lifetime provided by battery manufacturer is obtained under a standard and static operational condition, while in real-life application battery operates under variable operational conditions leading to different estimated battery lifetime due to the different degradation behavior over battery operation and storage [17, 24–26]. In other words, battery lifetime in real life applications highly depends on how battery operates and what services it provides to the electric grid. Thus, to increase the battery life through proper battery operation control strategies, full understanding of battery ageing influence parameters is essential. Electrochemical degradation of battery cells is a complex phenomenon and is determined by a combination of mechanisms that influence the electrodes and electrolyte [27–29]. The ageing mechanisms are different at the cathode and anode and typically more notable at the anode [30]. The main ageing mechanisms of Li-ion batteries include Loss of Li Inventory (LLI) and Loss of Active Material (LAM) [27,31]. LLI refers to the consumption of lithium ions due to growth of solid electrolyte interface (SEI) layer, decomposition reactions, and lithium plating. LAM denotes the fact that active materials of anode and cathode are no longer available due to particle cracking, graphite exfoliation, structural disarranging, loss of electrical contact due to passivation surface layers [32–34]. The evaluation of the impact of the LLI and LAM on the degradation of different battery cell chemistry have been studied by literature. For instance, Baure et al. [35,36] implemented the incremental capacity analysis method to further characterize the ageing effects occurring in the cells used in Ref. [37]. The results showed that the effect of the different degradation processes, e.g. LAM on the positive electrode of LCO or NCA, LAM on negative electrode and LLI are highly dependent one the test conditions. Results indicated that capacity loss of the full cell is dominated by LAM on negative electrode. It is assumed that with increased cell age LAM on positive electrode of NCA can become the dominant aging process under specific cycle aging conditions leading to an increased capacity fade [36].

The most common ageing mechanisms which are responsible for capacity fade of Li-ion battery cells and the corresponding stress factors are summarized as below [27,38–41].

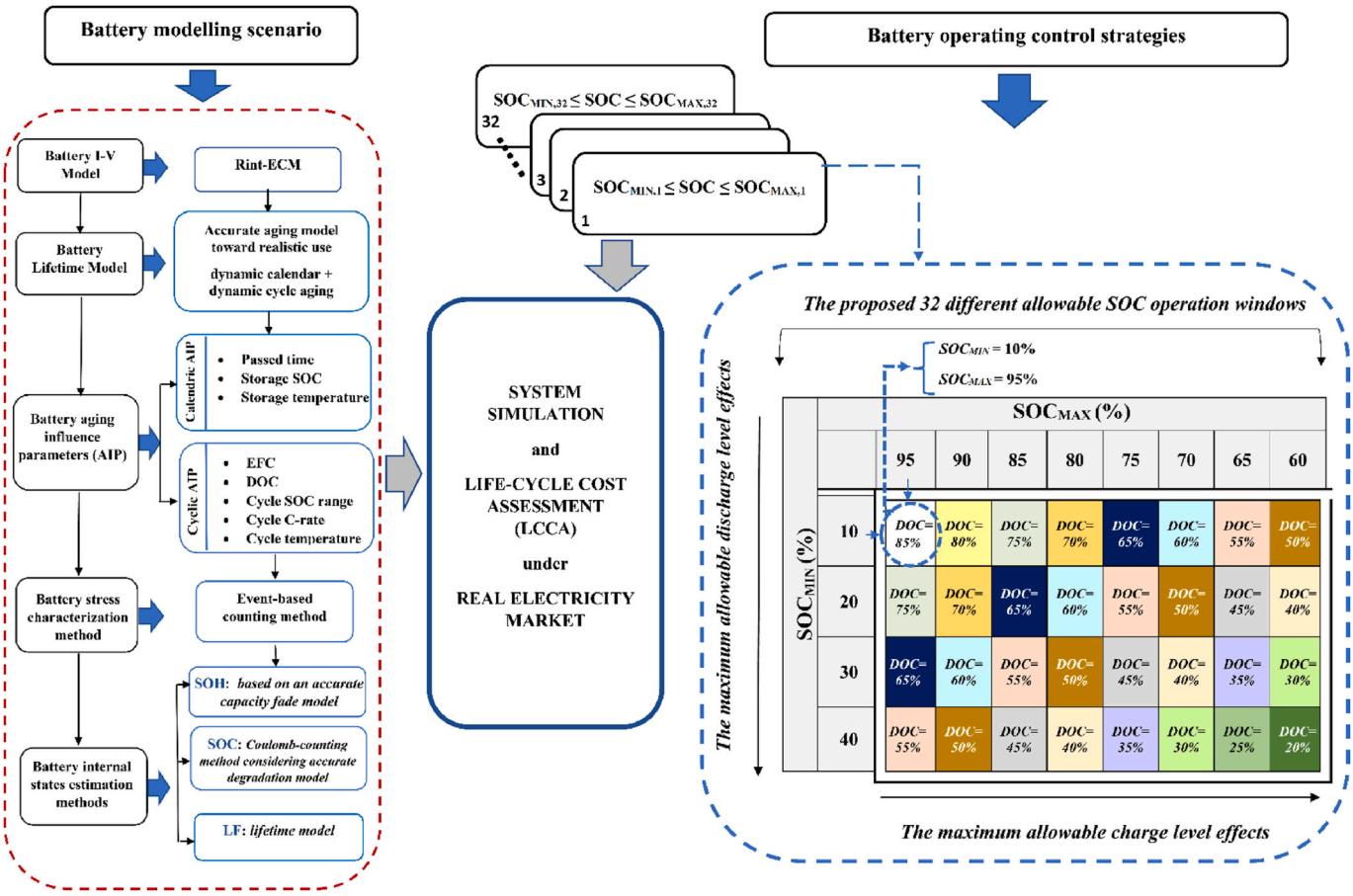

Fig. 1. Flowchart of the proposed strategy for the battery simulation conducted for the current case study.

(1) *Electrolyte decomposition, SEI formation and growth*: it causes loss of Li and is influenced by high SOC and high temperature.
(2) *Volume changes during cycling*: it leads to the loss of active material and is enhanced by a high depth of cycle (DOC) and high C-rate.
(3) *Cracking formation from solvent co-intercalation and gas evolution*: it causes loss of Li and the exfoliation of the graphite anode and is influenced by overcharge.
(4) *Binder decomposition*: it results in a loss of cyclable Li and loss of mechanical strength and is enhanced by high SOC and high temperatures.
(5) *Corrosion and Li-plating*: it causes a loss of cyclable Li, and possible unbalanced potential between cells. It is influenced by high SOC, overcharge, low temperatures, high C-rate.

Accordingly, each ageing mechanism is influenced by external factors. The most influential factors on capacity degradation include the temperature, the depth of cycle (DOC), the current rate (C-rate), and the SOC level [25,26,40,42]. Accordingly, an accurate battery capacity fade and lifetime model, which considers all possible ageing influencing parameters is essential for proper battery management system to predict the Li-ion degradation behavior under dynamic operational conditions. With regards this fact that Li-ion batteries age both during use (cyclic degradation) and during storage (calendric degradation) [43], an ageing model should be a superposition of calendric and cyclical ageing models [17,25,26]. Many studies on the estimation of calendric and cyclic degradation behavior of LFP/C batteries have been developed by considering the ageing stress factors; Among the calendric degradation models, the models introduced by Refs. [26,34-50] consider the dependency of calendric capacity fade on the storage SOC and temperature; however, the calendric degradation models proposed by Refs. [44,45,48,49] are valid only under constant storage SOC and temperature. Moreover, the models introduced by Refs. [46,50] are valid under dynamic storage temperatures but only at a constant SOC. Therefore, these models cannot predict the calendric ageing of batteries in applications that have dynamic operational profiles. Sarasketa-Zabala et al. [47] and Neuman et al. [25] proposed calendric ageing models that are valid under varying operational conditions. However, although acceptable prediction errors, the capacity fade models presented by Sarasketa-Zabala et al. [47] lack a customizable physio-chemical parameters and parameter fitting procedure. Conversely, Neuman et al. [25] proposed a high-accurate calendric ageing model that is valid under variable storage conditions, i.e., varying storage temperatures and SOCs. This model is used in the current study as the "towards realistic use" calendric ageing model. Among the cycling ageing models, many studies have proposed estimation models by considering the specific cycling ageing influence parameters [26,45,48-53]. Most of the studied cycling ageing models are function of the temperature and C-rate, and some of them consider DOC and SOC windows. Only the cycling ageing models proposed by Neuman et al. [26] and Wang et al. [52] were tested with dynamic profiles. However, the cycling ageing model presented by Neuman et al. [26] is a high-precision model that considers all possible ageing influencing parameters, such as the temperature, C-rate, and DOC and SOC window of a battery, and was developed based on a long-lasting experiment and systemically validated with dynamic load profiles. It is worth mentioning that in Ref. [26], in order to obtain the pure cycle aging, the respective calendar aging was subtracted from the cycle aging measurement values, accordingly the average SOC of the cyclization is the respective influence parameter of the underlying calendar aging. This model is employed in the current case study as the "towards realistic use" pure cycling ageing model.

Table 1
Description of the indicators in the current study.

Indicators	Objectives
• Hourly profile of calendric, cyclic and total degradation rates over battery life • Battery lifetime (LF) • Battery revenue • Battery life cycle cost assessments (LCCA) under real power market data illustrating with two indicators as below: o Economic view: battery life cycle cost (LCC) o Techno-economic view: battery net present value (NPV)	• What are the impacts of different battery SOC control strategies on the "indicators'' for a grid-connected residential application? • What are the impacts of electricity spot price, battery price, discount rate on the "indicators'' given the different SOC control strategies?

There are numerous studies evaluated the economic, as well as techno-economic viability of battery storage in different stationary applications, each of which assess their systems considering several simplified assumptions about the estimation of battery performance, degradation, and lifetime. For instance, studies such as those in Refs. [12,54-63] assumed that the battery current-voltage characteristics, battery capacity and lifetime were independent of battery operation; Moreover, studies such as those in Refs. [64–70] assumed that battery capacity is life-independent and also estimated the battery lifetime through several lifetime model neglecting the impact of battery degradation. Furthermore, some studies such as those in Refs. [15,71-74] predicted the battery lifetime and capacity fade considering simple ageing models neglecting ageing influence parameters. Few studies evaluated their system considering the impact of both calendric and cyclic degradation as the fully dependent on operating parameters. A recent published paper [17] explicitly evaluated techno-economic viability of battery in a stationary application under three different battery ageing models, highlighted that a more realistic techno-economic assessment is achieved under a realistic battery ageing model, while ignorant or incorrect estimation of battery capacity fade result in improper estimation of battery lifetime and techno-economic assessment. However, there is still an open problem that how to run batteries in a practical, and economic way to prolong battery lifetime and to make batteries a more viable technology in real electricity market from life cycle cost assessment (LCCA) perspective. As already mentioned, both calendric and cyclic degradation rates of battery strongly depend on the parameters such as battery charge/discharge rate, storage state-of-charge (SOC), depth-of-cycle (DOC), and operating temperature, each of which needs to be controlled through battery operating control strategies to be within proper ranges. Accurate information about which battery operating control strategies cause a high degradation rate can help to improve battery operation and extend the battery lifetime which lead to less frequent replacement in the application, and consequently economic profit. In most stationary applications, temperature is regulated by an air conditioning system to be within suitable bounds. Moreover, in real-life applications, knowing which SOC operation window cause a low degree of capacity fade during both storage and operation can prolong battery life and still is an explore question; To the best of authors knowledge, this issue was not explicitly addressed by the literature in stationary battery applications area. This paper aims to fill this research gap by introducing different operating control strategies analyzing the importance of different SOC control strategies on battery life longevity and its techno-economic viability in energy arbitrage application.

The main contributions of the present study are summarized as follows.

- Understanding the importance of battery operating control strategies on improving cyclic and calendric degradation rates, the lifetime and consequently techno-economic profitability of a battery system for arbitrage operation in day-ahead market. It should be noted that finding the maximum profit from energy arbitrage application can be framed as an optimization problem and is out of scope of this study, hence, a straightforward energy arbitrage model is implemented.
- As illustrated in Fig. 1 and Table 1, this study evaluates the different operating control strategies analyzing 32 different allowable SOC operation windows, each of which is separately given to the system simulation for controlling the (a) maximum allowable charge level (2) maximum allowable discharge level, and (3) maximum useable battery capacity, to evaluate at which SOC operation window the system simulation results in a harmless battery operation and more beneficial system in real power market from LCCA perspective.
- A battery modelling scenario is implemented which is able to properly estimate battery performance, i.e. voltage-current characteristics, capacity degradation, lifetime and battery internal states, i.e. SOC, and state-of-health (SOH) under dynamic operational conditions which are important factors for a proper battery management in real-life applications. The implemented ageing model is based on a realistic capacity fade model which estimate both cyclic and calendric capacity fades considering all possible ageing influence parameters.
- An operational strategy, which system can benefit from the dynamic electricity price, is conducted to simulate the operation of the grid-connected battery system given different operating control strategies. In the evaluation, techno-economic indicators such as battery life cycle cost, revenue, self-sufficiency ratio and battery net present value are taken into account.
- Sensitivity analysis is carried out to determine the sensitivity of economic results to the economic assumptions such as electricity spot price, the discount-rate, and the battery price per energy content.

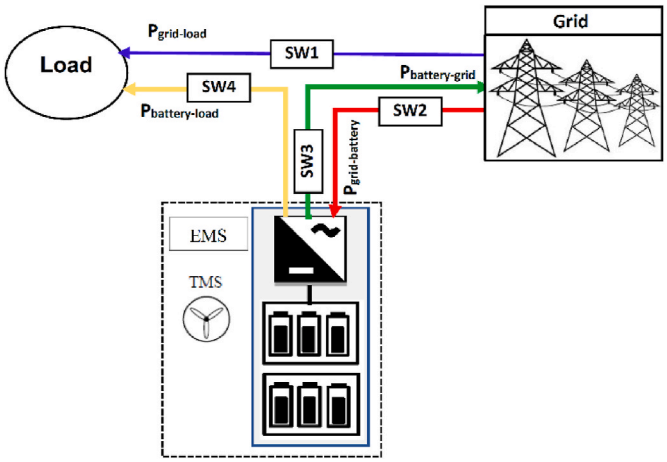

Fig. 2. Schematic of the studied grid-connected battery system.

The paper is organized as follows. Section 1 is the introduction. Section 2 describes the methods; Section 3 presents the results and discussion; and Section 4 summarizes the results and draws conclusions.

2. Methods

Section 2.1 presents the schematic layout of the studied system. Sections 2.2 and 2.3 describe the case study and its local electricity market, respectively. Section 2.4 illustrates the battery system modelling scenario. Section 2.5 introduces the problem definition and life cycle cost analysis. Finally, Section 2.6 presents the operative hypotheses and system operational strategy.

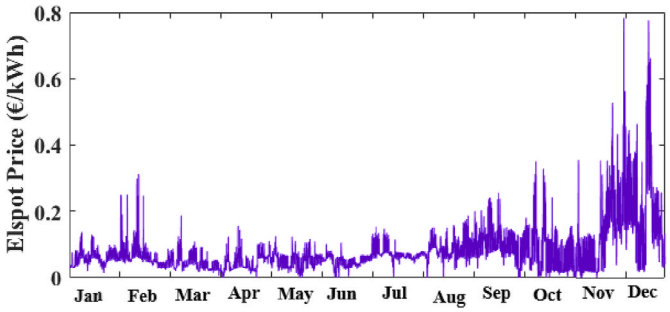

Fig. 3. The hourly profile of the Elspot price including VAT, 2021 [70].

2.1. System schematic layout

The schematic of the studied residential grid-connected battery system is shown in Fig. 2. The system consists of the AC battery with its own built-in inverter allowing the battery to directly convert its stored DC power into AC power; a temperature controller to regulate the battery system temperature; an electric grid, and a load. In short, the system exploits the price arbitrage strategy which consists in charging the battery during off-peak hours and discharging the stored electricity during high price periods.

2.2. Case study

This study is conducted for a typical Swedish family house, equipped with district heating, with the annual electricity consumption of 4300 kWh, which represents an average four-to-six-person household located in Västeras, Sweden. The hourly electricity consumption over one year is recorded by electric meters and the data received from the household owner.

2.3. Local electricity market

One of the flexible electricity-pricing schemes is real time pricing (RTP) which the customer electricity prices can vary hourly, and electricity users can manage their power consumption taking advantage of the price arbitrage. The retail electricity price in Sweden depends on factors including client types, areas, local electricity market, taxes, etc. [75]. For the studied residential case study, the retail electricity price ($El_{r,i}$), as shown in Eq. (1), can be decomposed into one variable component, namely Electricity Spot Price, and one fixed component, namely Fixed fee. The Electricity Spot Price (ElSpot price) is the day ahead hourly price from the bidding electricity market Nord Pool [76]. The fixed fee includes energy tax, electricity transfer fee, value added tax (VAT), etc. The exported electricity is sold at the wholesale price, as shown in Eq. (2), which takes the ElSpot price, and some subsidies such as grid benefit compensation and tax reduction into account. Fig. 3 shows the hourly Elspot price (c_i) in 2021 related to bidding area SE3 in Sweden. The values of c_2, c_3, c_4, c_5 indicated in Eqs. (1) and (2) are summarized in Appendix (Table A1).

$$EL_{r,i}\left(\frac{€}{kWh}\right) = c_i + c_2 + c_3 \tag{1}$$

$$EL_{w,i}\left(\frac{€}{kWh}\right) = c_i + c_4 + c_5 \tag{2}$$

2.4. Battery system

One of the variants of Li-ion batteries which has received more attention for use in stationary application is Lithium-iron phosphate (LFP/C) due to its high safety, long lifetime, high charging/discharging rate, long cyclability and nontoxic material. Accordingly, in this study, LPF battery with the technical specifications [77] illustrated in Appendix (Table A2) is implemented. subsections 2.4.1-2.4.3 describe the battery modelling processes, internal states estimation methods, and operating control strategies, respectively.

2.4.1. Battery modelling scenario

The battery current-voltage relationship is represented by the Rint electrical model [78]. The model describes the charging and discharging terminal voltages as a function of the dynamic operating conditions, as illustrated in Eqs. (3) and (4). A full explanation of the studied battery performance model can be found in author's previous work [17].

$$V_{ch,i}(SOC_i, T, I_i) = OCV_{ch}(SOC_i, T, I_i) + I_{ch,i} \times R_{ch}(SOC_i, T, I_i) \tag{3}$$

$$V_{dch,i}(SOC_i, T, I_i) = OCV_{dch}(SOC_i, T, I_i) + I_{dch,i} \times R_{dch}(SOC_i, T, I_i) \tag{4}$$

The battery lifetime and capacity fade in this study are presented by a "towards realistic use" ageing model which was obtained and validated under dynamic stress profiles by Naumann et al. [25,26].

The total battery capacity fade at each time interval is described by Eq. (7) which is obtained by superimposing the calendric capacity fade model, as shown in Eq. (5), and pure cyclic capacity degradation model, as shown in Eq. (6). For more illustration, the model estimates capacity degradation during both storage and operation as function of all possible calendric and cyclic ageing influence factors, such as storage state of charge, cycle depth, elapsed time since the BOL, full equivalent cycle (FEC), cycle charge/discharge rate. A full description of the implemented ageing model and how to apply the model under varying operational conditions are given in [17].

$$C_{\text{fade,cal}_i}(SOC, time) = \left(\alpha_1 (SOC - 0.5)^3 + \alpha_2\right).\, time^{0.5} \tag{5}$$

$$C_{\text{fade,cyc}_i}(C_{rate}, DOC, FEC) = (\beta_1.\, C_{rate} + \beta_2) \times \left(\gamma_1 (DOC - 0.6)^3 + \gamma_2\right) \times (FEC)^{0.5} \tag{6}$$

$$C_{\text{fade,tot}_i}(SOC, time, C_{rate}, DOC, FEC) = \left(C_{\text{fade,cal}_i}(SOC, time) + C_{\text{fade,cyc}_i}(C_{rate}, DOC, FEC)\right) \times C_{\text{batt,BOL}} \tag{7}$$

2.4.2. Battery internal estates estimation methods

The battery SOC and state-of-health (SOH) are two important battery internal states which indicate the level of charge remaining in battery and the level of battery degradation, respectively, and need to be tracked through proper state prediction methods. In this study, SOC at each time interval Δt_i is estimated by Coulomb counting method as illustrated in Eq. (8). The case of $(S_2{+}S_{3,4}) \leq 1$ in Eq. (8) means battery is not permitted to charge and discharge at the same time. By virtue of this fact that Li-ion batteries characterized by the low self-discharge per month [79], the impact of Li-ion self-discharging is neglected in our calculations. The battery SOH at each time interval Δt_i is represented by Eq. (9). The battery lifetime is defined by the elapsed time since BOL at which the battery SOH reaches to end-of-life battery capacity as illustrated in Eq. (10).

$$SOC_{i+1} = SOC_i - s_2 \frac{\int I_{ch,i}\, di}{SOH_i C_{batt,BOL}} + s_{3,4} \frac{\int I_{dch,i} di}{SOH_i C_{batt,BOL}} \quad \begin{cases} I_{ch,i} < 0 \\ I_{dch,i} > 0 \\ S_2 + S_{3,4} \leq 1 \end{cases} \tag{8}$$

$$SOH_i = \frac{C_{\text{batt}_i}}{C_{\text{batt,BOL}}} \times 100 = \frac{C_{\text{batt,BOL}} - C_{fade,tot_i}}{C_{batt,BOL}} \times 100 \tag{9}$$

$$LF\ (\text{years}) = \frac{i_{SOH_i \leq 80\%}}{8760} \quad i = 1, \ldots, \text{project lifetime (hr)} \tag{10}$$

2.4.3. Battery operating control strategies

Battery operating control parameters, as shown in Eq. (11), are important for the proper battery management granting that the battery

operates within allowable criteria. The parameters are battery end-of-life (EOL) indicator, battery capacity and the maximum battery charge and discharge power, and battery SOC operation window.

$$\begin{cases} SOH_i \le \alpha_{\text{Replace}} \rightarrow EOL_{\text{batt}} \quad \rightarrow \quad \alpha_{\text{Replace}} = 80\% \\ P^{\text{ch}}_{\text{min},i} \le P_{\text{batt},i} \le P^{\text{dch}}_{\text{max},i} \quad \rightarrow \quad \begin{cases} P^{\text{ch}}_{\text{min}} = -C_{\text{batt}_i} \times (SOC_{\max} - SOC_{\min}) \times \dfrac{C}{6} \\ P^{\text{dch}}_{\text{max}} = C_{\text{batt}_i} \times (SOC_{\max} - SOC_{\min}) \times \dfrac{C}{6} \end{cases} \\ SOC_{\min} \le SOC_i \le SOC_{\max} \quad \rightarrow \quad \begin{cases} SOC_{\min} = \{10\%, 20\%, \ldots, 40\%\} \\ SOC_{\max} = \{95\%, 85\%, \ldots, 60\%\} \end{cases} \end{cases} \tag{11}$$

In this study, $\delta_{\text{Replace}} = 80\%$ is used as the battery replacement indicator, which indicates that the battery EOL occurs in the application when the battery SOH reaches 80%, matching the warranty condition of the LFP/c battery. In current study, a 4 kWh battery is used and its maximum C-rate is assumed to be $\frac{1}{6}$ for both charging and discharging, which means battery is allowed to charge and discharge its useable capacity over 6 h. The battery SOC operation window defines the minimum and maximum allowable battery discharge and charge levels, respectively. Altering the allowable SOC operation window leads to the alteration of the maximum allowable depth of cycle, i.e., alteration of the maximum useable capacity, which affects the cyclic degradation rate, moreover it forces the battery to operate within a specific SOC level, which affects the calendric degradation rate. So, a proper SOC operation window leads to proper battery operating control and management, and lifetime improvement. In order to have a comprehensive evaluation, a wide range of allowable SOC operation windows each of which with specific threshold values, as shown in Eq. (11) and Fig. (1), are assumed for controlling (a) the maximum allowable charge level, i.e., maximum SOC, (b) the maximum allowable discharge level, i.e., minimum SOC, and (c) the maximum allowable depth of cycle of battery, i.e., useable battery capacity. In this assessment, for examining the impact of the maximum allowable charge level, a wide range of the threshold values from 95% to 60% with 5% interval are considered. Moreover, for controlling the maximum allowable discharge level, different threshold values from 10% to 40% with 10% interval are assumed; it should be noted that threshold values for lower SOC limit are altered with 10% interval instead of 5% as considered for upper SOC limit, due to this fact that experiments by authors showed that minimum SOC is less sensitive than maximum SOC. All the assumed SOC operation windows are set to cover a wide range of threshold values for the maximum allowable depth cycle from 20% DOC to 85% DOC with 5% interval.

2.5. Problem definition and life cycle cost assessment parameters

The main goal of this study is to understand the importance of the proper battery operating control strategies, considering a wide range of SOC operation windows, on calendric and cyclic degradation rates, the lifetime longevity and consequently techno-economic profitability of the battery system for price arbitrage application in day-ahead market.

Life-cycle cost analysis (LCCA) is a tool to determine the most cost-effective option among different competing alternatives. Accordingly, in this study, two economic indicators, namely life cycle cost (LCC), which evaluates the system from economic point of view, and net present value (NPV), which evaluates the system from techno-economic point of view, are considered.

As shown in Eq. (12), the LCC of system represents the present value of total cost of the system ownership over the project lifetime including initial investment cost ($\text{ICC}_{\text{battery}}$), maintenance and operation costs, and replacement costs of the battery within the project lifetime (25 years). It is worth mentioning that LCC does not take the system income into account. In contrary, as shown in Eq. (14), NPV represents the economic benefits of the system, which takes into account the present values of system costs and revenues within the system lifetime. To convert all cash flows into present equivalent values over the system's lifespan, the LCC and NPV approaches use the discount rate. In this study, the real discount rate is chosen as 4% by considering the current loan rate in Sweden [80].

Eq. (15) summarizes the system revenue over project lifetime, which can be categorized into two parts. The first part is the electricity reduction revenue, which comes from the difference between the peak electricity prices (in which the load met by the battery ($P_{batt\text{-}load,k} \times El_{r,i}$)), and the off-peak electricity prices (in which the electricity is bought from the grid for charging the battery ($P_{grid\text{-}batt,k} \times El_{r,i}$)). The second part is the electricity export revenue, which means that the surplus electricity will be exported to the grid ($P_{batt\text{-}grid,\ k} \times El_{w,i}$). The exported electricity is sold at wholesale price. Another indicator is the self-sufficiency ratio (SSR), as shown in Eq. (16), presenting how much of the total household consumption (E_{load}) is supplied by the battery system ($E_{out,battery}$).

$$LCC_{battery} = ICC_{battery} + \sum_{n=1}^{\text{Projectlifetime}} \frac{C_{O\&M,n}}{(1+\text{Interest}_{\text{rate}})^n} + \sum_{r=1}^{R} \frac{ICC_{battery}}{(1+\text{Interest}_{\text{rate}})^{r.\ LF}} - \frac{\text{Salvage value}}{(1+\text{Interest}_{\text{rate}})^{\text{Projectlifetime}}} \tag{12}$$

$$\text{Salvage value} = \left(1 - \frac{C_{fade,tot_x}}{(1-\alpha_{Replace})}\right) \times ICC_{battery}\ ;\ x = (\text{used lifetime at the end of project}) \times 8760 \tag{13}$$

$$NPV = \sum_{n=1}^{\text{Projectlifetime}} \frac{\text{Revenue}_n}{(1+\text{Interest}_{\text{rate}})^n} - LCC_{battery} \tag{14}$$

$$\text{Revenue}_{tot} = \sum_{n=1}^{\text{Projectlifetime}} \text{Revenue}_n = \sum_{n=1}^{\text{Projectlifetime}} \left(\left(\sum_{i=1}^{8760} P_{batt-load,i} \times El_{r,i} \right)_n - \left(\sum_{i=1}^{8760} P_{grid-batt,i} \times El_{r,i} \right)_n + \left(\sum_{i=1}^{8760} P_{batt-grid,i} \times El_{w,i} \right)_n \right) \tag{15}$$

$$SSR_{battery} = \sum_{n=1}^{\text{Projectlifetime}} \left(\frac{E_{out,battery,n}}{E_{load,n}} \right) \times 100 \tag{16}$$

2.6. Operative hypotheses and system operational strategy

In this study, a straightforward operational strategy, which system can take advantages from the dynamic electricity price, is proposed to simulate the operation of the studied residential grid-connected battery system over the project lifetime under 32 different operating control strategies. With regards the data availability and computational time, selecting a suitable size of data records (from a single day to a whole year) highly influences the final techno-economic assessment of energy systems [81]; accordingly, in this study, to ensure a realistic assessment, the system simulation is carried out given the hourly data records over whole year. The input data received by the system operational strategy are the hourly electricity consumption, dynamic real-time electricity price profile, battery capacity, the initial values of the battery SOC and SOH, and battery the operating control parameters, i.e. battery charge/discharge rates, battery EOL indicator, battery allowable SOC operation window, as illustrated in section. 2.4. The output data of the operational strategy are hourly system operations data, such as the battery power flow, SOC, SOH, the battery calendric and cyclic capacity fades and battery lifetime, and techno-economic indicators such as $\text{SSR}_{\text{battery}}$, $\text{Revenue}_{,\text{tot}}$, $\text{LCC}_{\text{battery}}$, NPV.

In the calculations, the following assumptions are made.

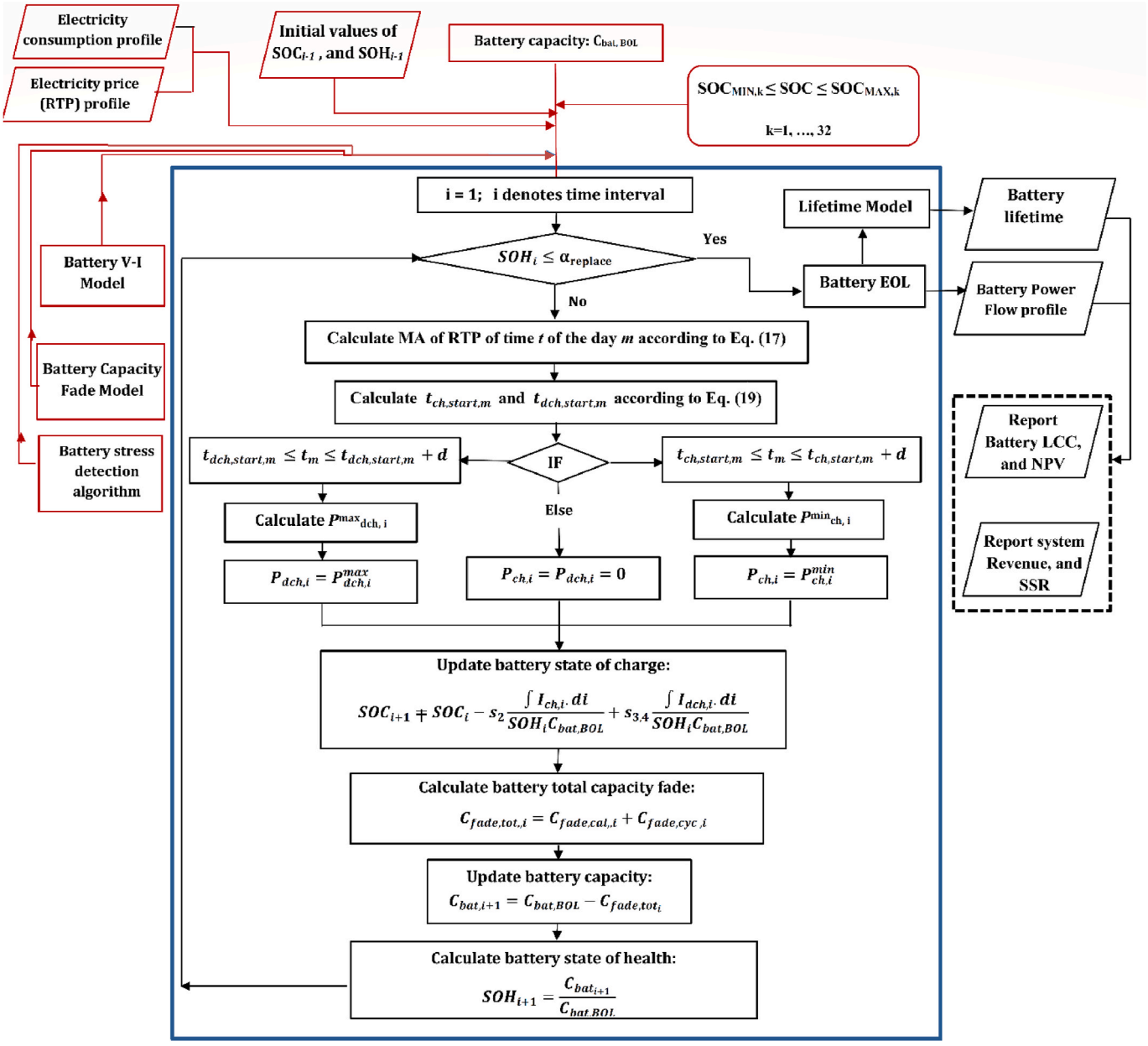

Fig. 4. The proposed simulation strategy.

- The system simulation is carried out on hourly basis assuming 25 years project lifetime in which the implemented annual hourly electricity price and consumption profiles remains unchanged over project lifetime.
- The battery charge/discharge rates are assumed constant and equal to C/6 in each time interval.
- Battery is charged and discharged only once a day in which the battery charge/discharge durations are assumed to be constant and equal to 6 h under all the 32 operating control strategies, i.e. the battery is allowed to charge and discharge its useable capacity during six low and high price hours, respectively.
- The battery lifetime is not a fixed value and depends on the battery operation in the system, estimated through the realistic ageing model which takes both cyclic and calendric degradations into account.
- The battery returns to the initial state of charge at end of each charge/discharge cycle.

Given each SOC operation window, the following is a brief description of the considered operational strategy as shown in Fig. 4.

- The 24-h ahead electricity price information is fed into the controller to determine system operation at time t of the day m. Accordingly, given each day-ahead real-time pricing (RTP) profile, the moving average (MA) of RTP prices in time t, corresponding to the charge/discharge duration d in the day m are calculated through Eq. (17). Where m is an index denoting the day of the year, d is an index denoting the charge/discharge duration, and t is an index denoting the hour of the day.

$$MA_{RTP_m}(t) = \sum_{k=t}^{t+d-1} RTP(k)/d \quad ; m = 1, \ldots, 365\ days; t = 1, \ldots, 24 - d + 1; d = 6hr \tag{17}$$

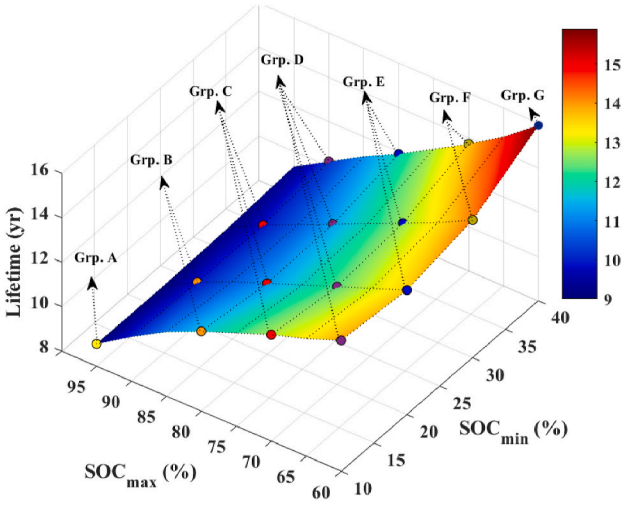

(a)

Fig. 5. Comparison of the (a) battery lifetimes, (b) self-sufficiency ratios, (c) ratios of the battery revenue to the initial investment cost, (d) battery life cycle costs, (d) battery net present values obtained under the 32 different SOC control strategies, relating to a battery capacity of 4 kWh operated under the fixed charge/discharge rates of C/6.

- Then, the minimum and maximum values of the MA RTP profile corresponding to the day m are calculated, as shown in Eq. (18), to determine the charge and discharge start time indicators corresponding to the day m as shown in Eq. (19).

$$MA_{RTP_{m,Min}} = Min(MA_{RTP_m}(t)); \quad MA_{RTP_{m,Max}} = Max(MA_{RTP_m}(t)) \tag{18}$$

$$t_{ch,start,m} = t_m @ MA_{RTP_{m,Min}};\ t_{dch,start,m} = t_m @ MA_{RTP_{m,Max}} \tag{19}$$

- If the time of the day m is within the allowable charge period of day m ($t_{ch,start,m} \le t_m \le t_{ch,start,m} + d$), the battery is charged with the low-price grid power at the maximum allowable charge rate.
- If the time of the day m is within the allowable discharge period of day m ($t_{ch,start,m} \le t_m \le t_{ch,start,m} + d$), the battery is discharged to support the demand as much as possible during high price period. If the maximum allowable discharge power is higher than the load, the excess power is sold to the grid. Otherwise, the deficit power is supplied by the grid
- At other times, the battery is neither charged or discharged and will be in the idle mode, and the demand is met by the grid.
- At the end of the algorithm, the following steps are completed.
  - The battery SOC is updated via the Coulomb counting method, as described in Section 2.4.2.
  - Through battery stress detection methods, the battery ageing influence parameters are detected, and both the calendric and cyclic capacity fades of the battery are calculated through the ageing models described in Section 2.4.1.
  - The battery capacity is updated based on the estimated capacity fade, and then the battery SOH level is updated based on the available battery capacity.
- The previously described procedure is consecutively repeated until the battery SOH reaches the predefined EOL criterion.

3. Result and discussion

In this section, first the impact of different SOC control strategies on the indicators are compared and discussed, then the sensitivity analyses on economic assumptions are carried out and discussed.

3.1. The impact of SOC control strategies on the studied indicators

Fig. 5a shows the estimated battery lifetimes until 80% capacity fade due to both calendar and cycle ageing, obtained from system simulation given the 32 SOC control strategies, relating to a fixed battery size (4 kWh) which operates with the charge and discharge rates of C/6, i.e. d = 6hr.

Fig.5b–e shows the corresponding self-sufficiency ratio (SSR), earned income over project life, the battery life cycle cost (LCC), and the net present value (NPV), obtained given the proposed strategies. To clarify the reason that why each SOC control strategy results in a different lifetime and techno-economic indicators, Fig. 6 shows the time variations of the calendric, cyclic, and total battery capacity degradations till battery EOL and also battery operating SOC histogram. For the sake of conciseness, in each of Fig.6a–b, only two SOC control strategies are shown as representative strategies. For example, Fig. 6a compares the degradation rate of two selected operating control strategy with same SOC_{min} (40%) to clarify the impact of increasing the level of SOC_{max} from 60% to 95% on the degradation rate. In contrast, Fig. 6b compares the degradation rate of the two selected operating control strategy with same SOC_{max} (60%) to clarify the impact of increasing the level of SOC_{min} from 10% to 40% on total ageing rate. It is worth mentioning that the total ageing under each modelling scenario is obtained by summing up the contributions of the accumulated cycling and calendric capacity fades.

It can be observed from Fig. 5a that given the same allowable discharge level, i.e. fixed SOC_{min}, those operating control strategies which set the allowable charge levels, i.e., SOC_{max}, to upper levels result in much shorter battery lifetimes. This originates from the facts that increasing the allowable charge limit from 60% to 95% SOC, allows the battery to operate with higher voltages which considerably enhances the rate of cyclic ageing (see the example in Fig. 6a) due to the operating with deeper cycle depths, moreover, it significantly enhances the rate of calendric ageing (see the example in Fig. 6a) due to the storage at higher

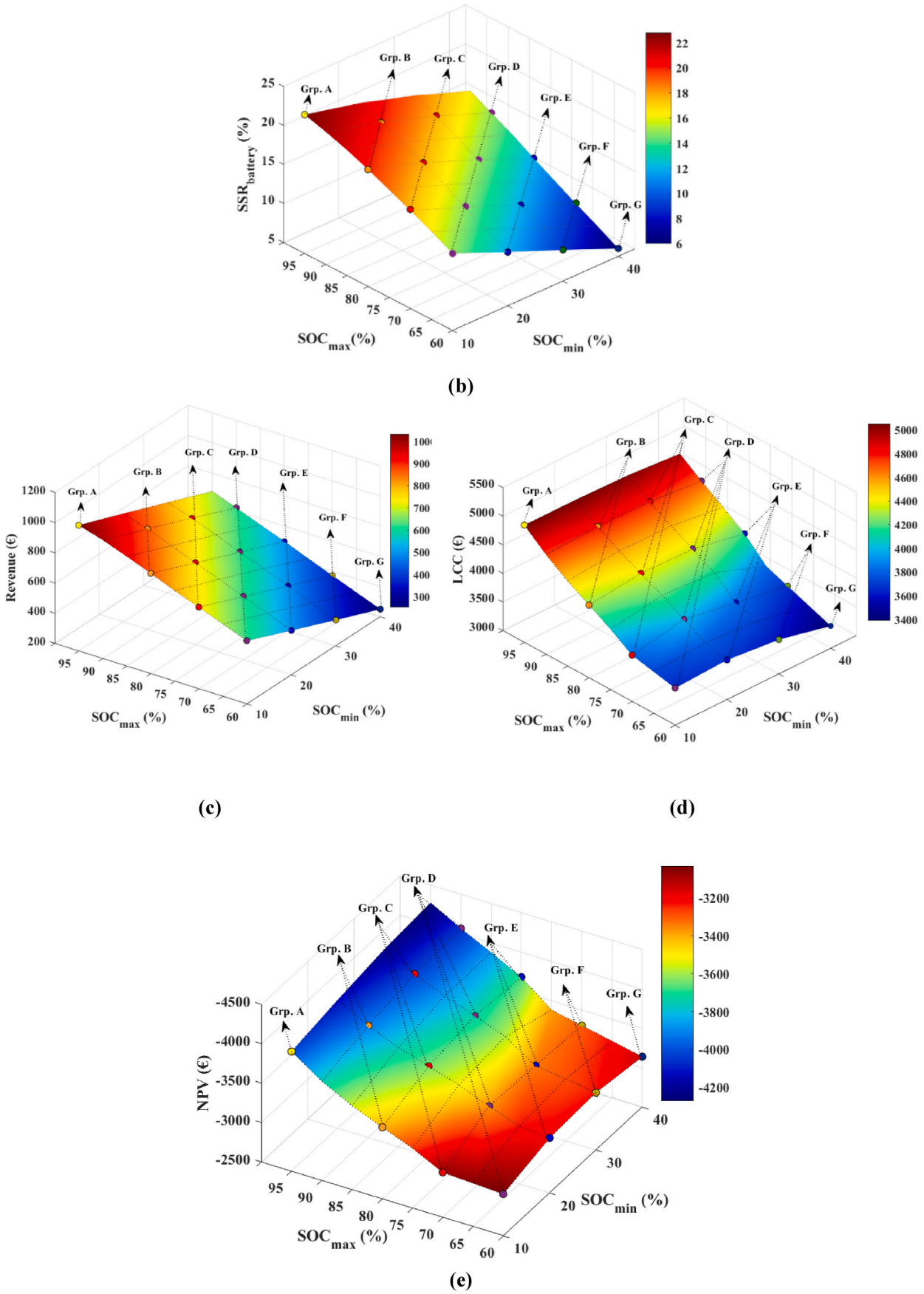

Fig. 5. (*continued*).

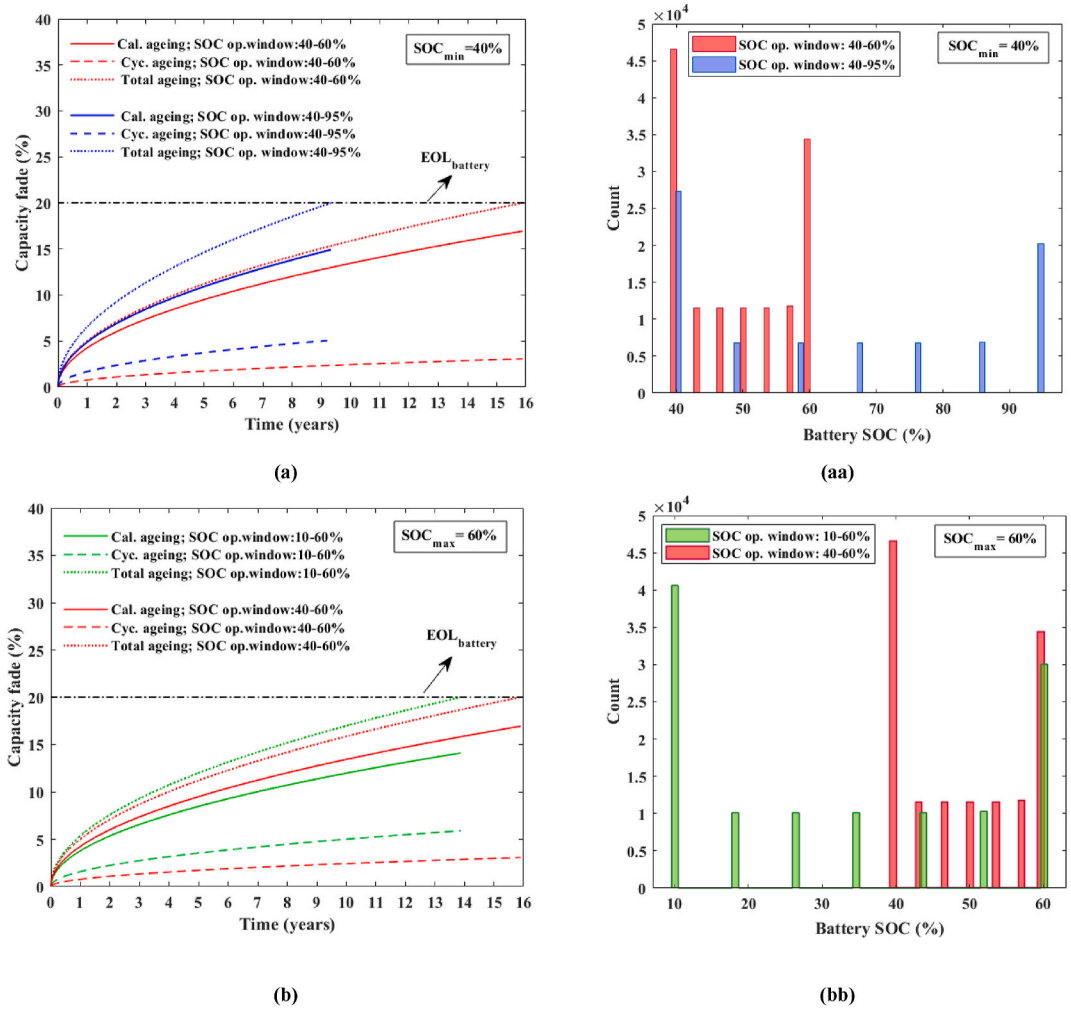

Fig. 6. The contributions of calendric and cyclic degradation to the overall capacity loss (left figures), and the SOC histogram over battery lifetime (right figures), relative to (a-aa) two representative strategies with the same SOC_{min} = 40%, (b-bb) two representative strategies with the same SOC_{max} = 60%.

SOC levels (see the example in Fig. 6aa), which both simultaneously lead to the faster degradation and consequently lead to the shorter battery lifetime, which negatively affect the life cycle cost. On the other hand, as shown in Fig. 5a, given the same allowable charge levels, i.e. fixed SOC_{max}, leveling up the allowable discharge levels, i.e. SOC_{min}, improves the battery life longevity. This is because of the fact that although increasing the allowable discharge level from 10% to 40%, increases the calendric degradation rate (see the example in Fig. 6b) due to storage at

Table 2
Detailed techno-economic simulation results related to seven categorized groups of solutions.

Group	Operational strategy (OS)	DOC (%)	SOC window	LF (yr)	LF changes vs. that of the worst OS (%)	Revenue (€)	LCC (€)	LCC changes vs. that of the worst OS (%)	NPV (€)	NPV changes vs. that of the worst OS (%)	Best OS of each group
A	OS. A	85	10–95%	9 (worst)	0	1033	5051 (worst)	0	−4018	0	OS. A
B	OS·B1	70	10–80%	11.6	+29%	865	4275	−15.4%	−3410	−15.1%	OS·B1
	OS·B2		20–90%	9.9	+10%		4783	−5.3%	−3918	−2.5%	
C	OS·C1	60	10–70%	12.8	+42.2%	742	3813	−24.5%	−3071	−23.6%	OS. C1 (2nd rank)
	OS·C2		20–80%	11.2	+24.4%		4379	−13.3%	−3637	−9.5%	
	OS·C3		30–90%	9.9	+10%		4770	−5.6%	−4028	+0.3%	
D	OS. D1	50	10–60%	13.9	+54.4%	620	3651	−27.7%	−3031	−24.6%	OS. D1 (1st rank)
	OS. D2		20–70%	12.4	+37.8%		3986	−21.1%	−3366	−16.2%	
	OS. D3		30–80%	11.3	+25.6%		4354	−13.8%	−3734	−7.1%	
	OS. D4		40–90%	10.2	+13.3%		4610	−7.3%	−3990	+1.1%	
E	OS. E1	40	20–60%	13.6	+51.1%	495	3694	−26.9%	−3199	−20.4%	OS. E1
	OS. E2		30–70%	12.7	+41.1%		3832	−24.1%	−3337	−17%	
	OS. E3		40–80%	11.9	+32.2%		4176	−17.3%	−3681	−8.4%	
F	OS·F1	30	30–60%	14.2	+57.8%	372	3601	−28.7%	−3229	−19.6%	OS. F1 (3rd rank)
	OS·F2		40–70%	13.7	+52.2%		3672	−27.3%	−3300	−17.9%	
G	OS. G	20	40–60%	15.9	+76.7%	250	3390	−32.8%	−3140	−21.9%	OS. G

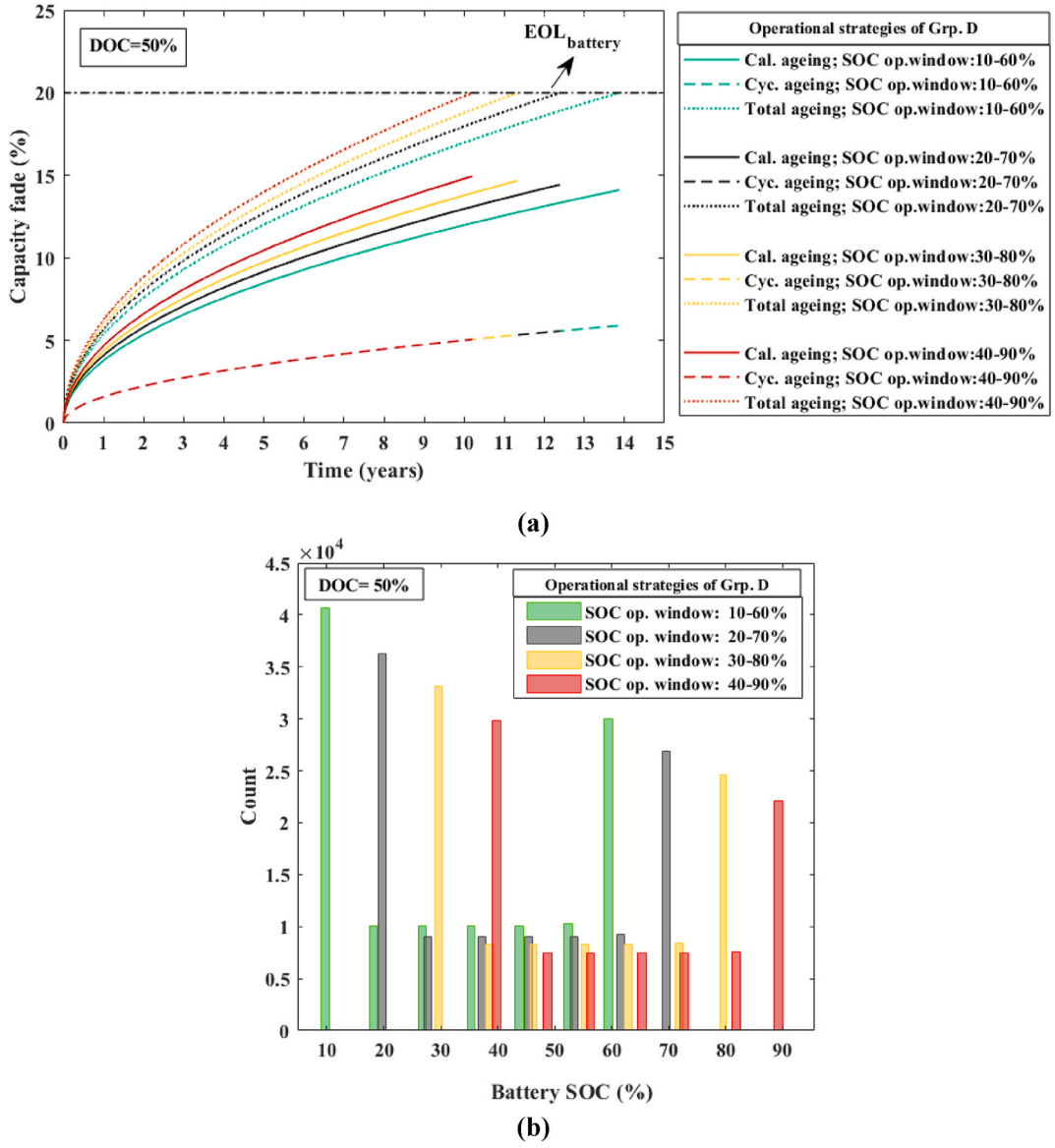

Fig. 7. (a) The contributions of calendric and cyclic degradation to the overall capacity loss, and (b) the SOC histogram over battery lifetime, relative to strategies of Grp. D which all have same depth of cycle of 50% with different SOC operation windows.

higher SOC levels (See the example in Fig. 6bb), it significantly decreases the cyclic degradation rate (see the example in Fig. 6b) due to the charge cycle with smaller depths which improve total degradation rate and positively affect the battery lifetime.

Accordingly, as shown in Fig. 5b–d, given the same SOC_{min}, the SOC control strategies with upper allowable charge limit, i.e. SOC_{max}, result in the much more expensive battery life cycle costs (LCCs) due to more battery replacements as a result of shorter lifetime, in contrast, the self-sufficiency ratio and the earned income over project lifetime increase due to the enhancement of the battery useable capacity, implying that battery is allowed to buy more from and sell more to the grid which increases profit obtained from the price arbitrage and deliver more to user which increases revenue from the grid reduction. On the other hand, the SOC control strategies with lower allowable discharge limit lead to life cycle cost decrease due to the less replacement as a result of longer lifetimes, in contrast, the self-sufficiency ratio and the earned income over project lifetime increase due to the smaller cycle depths. From techno-economic point of view, in can be observed from Fig. 4e that setting allowable charge level to lower level, i.e., from 95% to 60%, and also keeping allowable discharge levels at lower levels, i.e. from 40% to 10%, positively affects the net present value (NPV).

In order to compare the detailed techno-economic simulation results obtained under the 32 presented SOC control strategies, the seven groups of solutions namely Grps. (A)–(G) (as designated in Fig. 5) are selected as the representative solutions and illustrated in Table 2. It is worth mentioning that each group consists of the operating control strategies which have the same DOC but different SOC operation windows, investigating the importance of SOC ranges on the battery ageing and techno-economic assessments.

On the one hand, it can be observed from Table 2 and Fig. 5 that although the OS. A results in the highest income among all the proposed operating strategies, it is techno-economically the worst strategy leading to the shortest battery lifetime, the highest LCC and the lowest NPV. Moreover, it can be observed that the best techno-economic outcomes are obtained under the strategy OS. D1 leading to the 54.4% higher lifetime, 27.7% lower LCC, and 24.6% higher NPV, than those of the worst case. i.e. OS. A. Furthermore, as shown in Table 2, the OS. G results in the longest lifetime and the lowest LCC with the 76.7% higher lifetime 32.8% lower LCC than those of the worst strategy. i.e. OS. A, however, the OS. G is not the best strategy from techno-economic point

of view and ranked 3rd with 21.9% higher NPV compared to that of the worst case, due to leading to the lowest income.

On the other hand, to clarify the importance of the SOC ranges and their impacts on improving the lifetime and the techno-economic assessment, Grp. D, which consist of four strategies OS. D1-OS.D4, is taken as an example. Fig. 7 compares the calendric, cyclic, and total degradation rates of all four strategies of Grp. D, illustrating the impact of the alteration of the SOC window given the same DOC.

It can be observed that all four strategies of Grp. D led to the same income and self-sufficiency ratio, regardless of the different SOC windows, due to the same useable capacity and the charge cycles with same DOC of 50%. However, those lead to the different techno-economic results, in which alteration of the allowable SOC levels to the upper levels significantly decrease the battery lifetime from 13.9 yr (belonging to the OS. D1 with SOC window of 10–60%) to 10.2 yr (belonging to the OS. D4 with SOC window of 40–90%). The This originates from the fact that although the same cyclic degradation rate (see Fig. 7a, dash lines), the rate of calendric ageing increases as a result of the leveling up the SOC limits (see Fig. 7a, solid lines) due to the storage at higher SOC (see Fig. 7b) which lead to the electrolyte decomposition, side reaction between electrolyte and cathode, and lithium deposition. Accordingly, selecting the SOC operation window of (10–60%) i.e. OS. D1, improve the LCC and NPV by 26.2% and 31.6% compared to the SOC operation window of (40–90%) i.e. OS. D4, implying the importance of the proper selection of battery SOC control strategy.

3.2. Sensitivity analysis

The economic assumptions about the electricity spot price, the discount-rate, and the battery price per energy content can influence the economic assessments, leading to the different revenues, LCCs, and NPVs. A sensitivity analysis is carried out to determine the most influential parameter.

3.2.1. Sensitivity analysis on electricity market changes

As illustrated in section 2.3, all the results obtained on the basis of the electricity market price of the year 2021 which chosen based on the most recent full-year data availability. However, according to the electricity market price statistics, in 2020, due to the covid-19, the shutdown of economies and the heavy rainfall in the Nordics, Sweden's electricity price hit an all-time low at annual average price of 22.1 €/MWh (Stockholm area, SE3), around half the level that was the same time a year prior. Contrary, in 2021, particularly since the autumn of 2021 (i.e., Sep, Oct, Nov, and Dec), electricity prices showed unprecedently high electricity market prices across most of Europe, including in price areas Stockholm (SE3) with annual average electricity price of 66 €/MWh, 300.2% higher than that of 2020, as cold temperatures increased demand and gas prices in Europe continue to rise. In 2022, the Sweden's electricity spot prices have developed even more dramatically, in which the half-year's average electricity prices (i.e., from Jan–Jun) have jumped to 100.5€/kWh, an increase of about 238% compared to the same period a year prior. Correspondingly, statistics shows that since second half-year of 2021, Sweden's electricity prices is undergoing high electricity prices. Accordingly, as electricity market is undergoing rapid change, it should be studied to what extend the electricity market influence the techno-economic assessment, when electricity costs change. In this study, three different representative electricity spot price profiles, as illustrated below, are separately given to the system operational strategy as input to evaluate sensitivity of results to the uncertainty in electricity market prices.

- Electricity market price of year 2020, a representative of normal year with annual average electricity price of 21.2 €/MWh
- Electricity market price of year 2021, a representative year with increased electricity prices at the second-half year, with annual average electricity price of 66 €/MWh

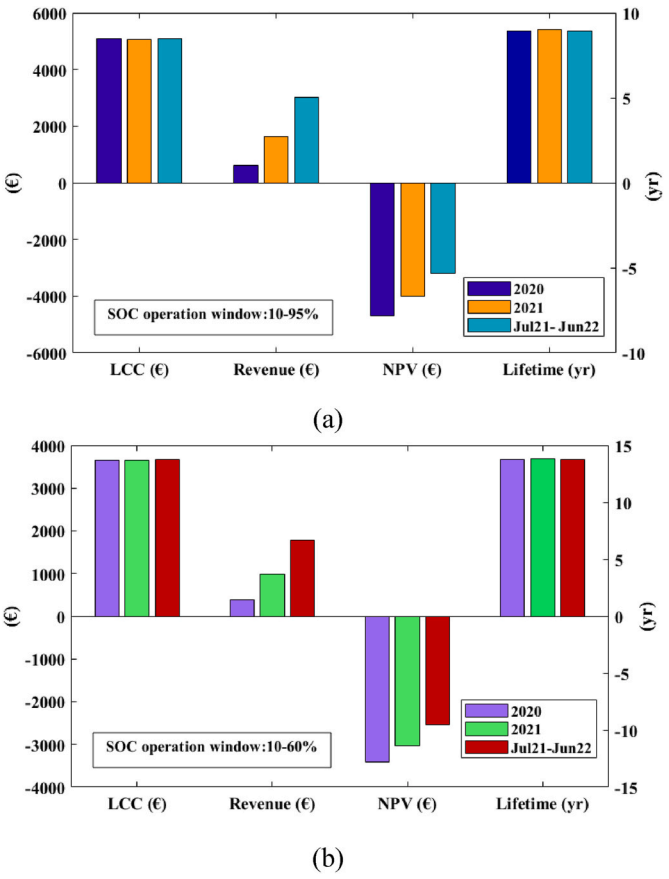

Fig. 8. Sensitivity of techno-economic results on three different electrcity price profiles, relating to (a) the worst SOC operation window; and (b) the best SOC operation window.

- Electricity market price of year Jul21_Jun22, a representative year which includes high electricity prices, with annual average electricity price of 95 €/MWh

Accordingly, given each battery control strategy, the system simulation is repeated three times with three different electricity price profiles. For the sake of conciseness, only two operational strategies, i.e. the worst control strategy (OS. A with SOC op. window: 10–95%) and the best control strategy (OS. D1 with SOC op. window: 10–60%), are selected for the current sensitivity analysis. Two examples shown in Fig. 8 which illustrates the sensitivity of results to the three different electricity price profiles. As shown in Fig. 8, under both strategies, the simulation based on electricity spot price of year 2020 and Jul21-Jun22, lead to 60% lower and 83% higher revenues compared to that of reference system (the system simulated based on the electricity spot price of year 2021) with no considerable changes in battery lifetime and LCCs. Accordingly, as shown in Fig. 7a, the simulation based on electricity spot price of years 2020 and Jul21-Jun22, lead to 17% higher (negative effect) and 20% lower (positive effect) NPVs compared to that of reference system, implying the importance of electricity price changes on techno-economic results. Moreover, it can be observed given all three different electricity price profiles, OS. D1 lead to the smaller negative NPV values, than those of OS. A.

3.2.2. Sensitivity analysis on economic assumptions

Fig. 9 shows the sensitivity of battery NPVs to the discount-rate and battery price changes. It can be observed that under both strategies of OS. A, and OS. D1, a 75% increase in the reference discount-rate, i.e., 4%, lead to 14% and 9% less negative (positive effect) NPV values than that of reference system, respectively. Moreover, a 75% decrease in the

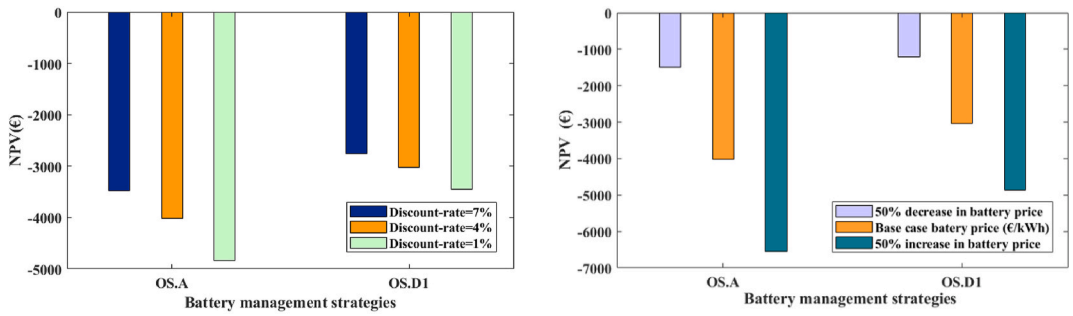

Fig. 9. Sensitivity of techno-economic results on discount rate and batery price, relating to (a) the worst SOC operation window; and (b) the best SOC operation window.

current discount rate, lead to 20% and 13% more negative (negative effect) NPV values than the reference system under OS. A, and OS. D1, respectively. Moreover, given different discount rates, OS. D1 always lead to smaller NPV values, compared to OS. A. As shown in Fig. 9b, a 50% increase in battery price results in high negative NPVs, with considerable difference between the best and the worst strategy. In contrast, a 50% decrease in battery price dramatically improve the NPV values with no considerable difference between OS. A, and OS. D1.

Overall, the results showed that battery management system highly influences the way to use batteries in an application. Given different battery SOC operating control strategies, system simulations lead to the different battery lifetimes, different calendric and cyclic degradation rates, and consequently different economic outcomes, highlighting that SOC operation windows, and depth of cycles are key influencing factors on battery lifetime and system profitability. The key results showed that strategies in which the battery is allowed to operate at low state-of-charge levels are less detrimental than those with higher state-of-charge levels, that noticeably improve battery lifetime, and profitability. The results of this study provide useful insights to the battery system designers and practitioners on how to use batteries in an efficient and practical way in order to extend battery lifetime, and properly size and optimize battery in real-life applications. Moreover, accurate information about which battery operating control strategies cause a high degradation rate can help researchers how to make battery working within long life and high-performance operating area depending on the study objective functions. The results of this study were evaluated for LFP/C batteries, however, the methodology implemented in this study are applicable for other types of batteries, other case studies.

4. Conclusion

The following conclusions can be drawn.

- From techno-economic point of view, simulation results showed that operating control strategies with low SOC levels are less detrimental than higher SOC levels. For more illustration, setting the allowable charge level to lower limits, i.e., from 95% to 60%, and also setting the allowable discharge levels to lower limits, i.e. from 40% to 10%, positively affect the battery NPV, in which the best strategy led to 30% less negative NPV compared to the worst strategy, highlighting the importance of the SOC operation window on improving the lifetime and the LCCA of a grid-connected battery system.
- Assuming the same allowable discharge level, the simulation results showed that SOC control strategies which set the allowable charge level, i.e., SOC_{max}, to lower limits from 95% to 60% led to the slower cyclic and calendric degradation rates and consequently much longer battery lifetime, which positively affect the life cycle cost and in contrast, negatively affect the earned income due to the diminution of the battery useable capacity, however, the improvement in battery degradation cost is noticeable compared to the revenue deterioration, resulting in considerable improvement in battery NPV. .
- Assuming the same allowable charge level, the simulation results indicated that although leveling up the allowable discharge levels, i.e. SOC_{min}, from 10% to 40% slightly improves the battery life longevity, which positively affect the battery life cycle cost, those result in considerable decrease in earned income, which negatively affect the battery NPV, because the improvement in battery degradation cost is imperceptible compared to the revenue deterioration.
- Assuming strategies with the same DOC but different SOC operation windows, the simulation results showed that alteration of the SOC window to the upper levels significantly decrease the battery lifetime. For more illustration take strategies belong to Grp. D, which all four strategies have same DOC but different SOC windows, as an example, it can be observed that all four strategies of Grp. D led to the same income regardless of the different SOC windows, however, those lead to the different techno-economic results in which alteration of the allowable SOC window from (40%–90%) to (10%–60%) increase the battery lifetime from 10.2 yr to 14 yr leading to 31.6% improvement in NPV.

Credit author statement

Masoume Shabani: Conceptualization, Methodology, Software, Formal analysis, Investigation, Writing – original draft, Writing – review & editing. Erik Dahlquist: Writing – review & editing. Fredrik Wallin: Writing – review & editing. Jinyue Yan: Formal analysis, Writing – review & editing.

Declaration of competing interest

The authors declare that they have no known competing financial interests or personal relationships that could have appeared to influence the work reported in this paper.

Data availability

The authors do not have permission to share data.

Acknowledgments

Authors would like to thank the support from the Swedish Energy Agency project ''Svensk Innovations-och Testaccelerator för E-mobilitet (SITE1), and from the Kowledge Foundation (kKKS) project'' flexibility through synergies of big data, novel technologies and innovative markets (FELEXERGY)'' and from ''Reduction and Reuse of energy with interconnected Distribution and Demand (R2D2) project.

Appendix A

Table A1
Characteristics of the studied Li-ion battery cells

Parameter	Value
Battery chemistry	$LiFePO_4/C$
Battery nominal voltage	3.2 V
Nominal capacity	2.5 Ah
Discharge cut-off voltage	2.5 V
Charge cut-off voltage (V)	3.6 V
Battery calendric lifetime until 80% capacity ($LF^{80\%}_{Calendar}$)	15 years
Battery cycle life until 80% capacity ($LF^{80\%}_{Cycle}$)	10,000 FEC
Battery maintenance cost (% of investment/year)	0.5%
Battery energy specific price (€/kWh)	570

Table A2
Electricity price components[1]

Symbol	Parameter	Value
C_i	ElSpot price	Illustrated in Fig. 3
C_2	Energy Tax, incl. VAT	0.45 SEK/kWh
C_3	Electricity transfer fee, incl. VAT	0.2875 SEK/kWh
C_4	Grid benefit compensation	0.035 SEK/kWh
C_5	Tax reduction	0.6 SEK/kWh

[1] The cost information in this study is presented in Euro. 1EUR = 10.526 SEK; The exchange rate among Euro, and SEK (currency in Sweden) are based on the average monthly rate in 2022. The rate currency is retrieved from http://www.x-rates.com/average/.

References

[1] Baure G, Dubarry M. Durability and reliability of EV batteries under electric utility grid operations: impact of frequency regulation usage on cell degradation. Energies 2020 May 15;13(10):2494.
[2] Dubarry M, Tun M, Baure G, Matsuura M, Rocheleau RE. Battery durability and reliability under electric utility grid operations: analysis of on-site reference tests. Electronics 2021 Jul 2;10(13):1593.
[3] Xing W, Wang H, Lu L, Han X, Sun K, Ouyang M. An adaptive virtual inertia control strategy for distributed battery energy storage system in microgrids. Energy 2021 Oct 15;233:121155.
[4] Palizban O, Kauhaniemi K. Energy storage systems in modern grids—matrix of technologies and applications. J Energy Storage 2016 May 1;6:248–59.
[5] Sepúlveda-Mora SB, Hegedus S. Making the case for time-of-use electric rates to boost the value of battery storage in commercial buildings with grid connected PV systems. Energy 2021 Mar 1;218:1–12. https://doi.org/10.1016/j.energy.2020.119447. 119447.
[6] Olabi AG, Wilberforce T, Sayed ET, Abo-Khalil AG, Maghrabie HM, Elsaid K, Abdelkareem MA. Battery energy storage systems and SWOT (strengths, weakness, opportunities, and threats) analysis of batteries in power transmission. Energy 2022 Sep 1;254:123987.
[7] IEA. Innovation in batteries and electricity storage. Paris: IEA; 2020. https://www.iea.org/reports/innovation-in-batteries-and-electricity-storage.
[8] Hesse HC, Schimpe M, Kucevic D, Jossen A. Lithium-ion battery storage for the grid—a review of stationary battery storage system design tailored for applications in modern power grids. Energies 2017 Dec;10(12):2107.
[9] Meng H, Geng M, Xing J, Zio E. A hybrid method for prognostics of Lithium-ion batteries capacity considering regeneration phenomena. Energy 2022 Aug 29:125278.
[10] Lin M, Yan C, Meng J, Wang W, Wu J. Lithium-ion batteries health prognosis via differential thermal capacity with simulated annealing and support vector regression. Energy 2022 Jul 1;250:123829.
[11] Núñez F, Canca D, Arcos-Vargas Á. An assessment of European electricity arbitrage using storage systems. Energy 2022 Mar 1;242:122916.
[12] Metz D, Saraiva JT. Use of battery storage systems for price arbitrage operations in the 15-and 60-min German intraday markets. Elec Power Syst Res 2018 Jul 1;160:27–36.
[13] Harrold DJ, Cao J, Fan Z. Data-driven battery operation for energy arbitrage using rainbow deep reinforcement learning. Energy 2022 Jan 1;238:121958.
[14] Staffell I, Rustomji M. Maximising the value of electricity storage. J Energy Storage 2016 Nov 1;8:212–25.
[15] Mayyas A, Chadly A, Amer ST, Azar E. Economics of the Li-ion batteries and reversible fuel cells as energy storage systems when coupled with dynamic electricity pricing schemes. Energy 2022 Jan 15;239:121941.
[16] Wankmüller F, Thimmapuram PR, Gallagher KG, Botterud A. Impact of battery degradation on energy arbitrage revenue of grid-level energy storage. J Energy Storage 2017 Apr 1;10:56–66.
[17] Shabani M, Wallin F, Dahlquist E, Yan J. Techno-economic assessment of battery storage integrated into a grid-connected and solar-powered residential building under different battery ageing models. Appl Energy 2022 Jul 15;318:119166.
[18] Dubarry M, Qin N, Brooker P. Calendar aging of commercial Li-ion cells of different chemistries–A review. Curr Opin Electrochem 2018 Jun 1;9:106–13.
[19] Han X, Lu L, Zheng Y, Feng X, Li Z, Li J, Ouyang M. A review on the key issues of the lithium ion battery degradation among the whole life cycle. ETransportation 2019 Aug 1;1:100005.
[20] Seng KH, Li L, Chen DP, Chen ZX, Wang XL, Liu HK, Guo ZP. The effects of FEC (fluoroethylene carbonate) electrolyte additive on the lithium storage properties of NiO (nickel oxide) nanocuboids. Energy 2013 Sep 1;58:707–13.
[21] Hofmann A, Höweling A, Bohn N, Müller M, Binder JR, Hanemann T. Additives for cycle life improvement of high-voltage LNMO-based Li-ion cells. Chemelectrochem 2019 Oct 15;6(20):5255–63.
[22] Miranda D, Gören A, Costa CM, Silva MM, Almeida AM, Lanceros-Méndez S. Theoretical simulation of the optimal relation between active material, binder and conductive additive for lithium-ion battery cathodes. Energy 2019 Apr 1;172:68–78.
[23] Zhang SS. A review on electrolyte additives for lithium-ion batteries. J Power Sources 2006 Nov 22;162(2):1379–94.
[24] Hu X, Xu L, Lin X, Pecht M. Battery lifetime prognostics. Joule 2020 Feb 19;4(2):310–46.
[25] Naumann M, Schimpe M, Keil P, Hesse HC, Jossen A. Analysis and modeling of calendar aging of a commercial LiFePO4/graphite cell. J Storage 2018 Jun 1;17:153–69.
[26] Naumann M, Spingler FB, Jossen A. Analysis and modeling of cycle aging of a commercial LiFePO4/graphite cell. J Power Sources 2020 Mar 1;451:227666.
[27] De Gennaro M, Paffumi E, Martini G, Giallonardo A, Pedroso S, Loiselle-Lapointe A. A case study to predict the capacity fade of the battery of electrified vehicles in real-world use conditions. Case Stud Transp Policy 2020 Jun 1;8(2):517–34.
[28] He R, He Y, Xie W, Guo B, Yang S. Comparative analysis for commercial li-ion batteries degradation using the distribution of relaxation time method based on electrochemical impedance spectroscopy. Energy 2022 Nov 7:125972.
[29] Šeruga D, Gosar A, Sweeney CA, Jaguemont J, Van Mierlo J, Nagode M. Continuous modelling of cyclic ageing for lithium-ion batteries. Energy 2021 Jan 15;215:119079.
[30] Birkl CR, Roberts MR, McTurk E, Bruce PG. Degradation diagnostics for lithium ion cells. J Power Sources 2017;341:373–86.
[31] Teliz E, Zinola CF, Díaz V. Identification and quantification of ageing mechanisms in Li-ion batteries by Electrochemical impedance spectroscopy. Electrochim Acta 2022 Sep 10;426:140801.
[32] Xu M, Wang X, Zhang L, Zhao P. Comparison of the effect of linear and two-step fast charging protocols on degradation of lithium ion batteries. Energy 2021 Jul 15;227:120417.
[33] Liu S, Winter M, Lewerenz M, Becker J, Sauer DU, Ma Z, Jiang J. Analysis of cyclic aging performance of commercial Li4Ti5O12-based batteries at room temperature. Energy 2019 Apr 15;173:1041–53.

[34] Stockhausen R, Gehrlein L, Müller M, Bergfeldt T, Hofmann A, Müller FJ, Maibach J, Ehrenberg H, Smith A. Investigating the dominant decomposition mechanisms in lithium-ion battery cells responsible for capacity loss in different stages of electrochemical aging. J Power Sources 2022 Sep 30;543:231842.
[35] Baure G, Dubarry M. Battery durability and reliability under electric utility grid operations: 20-year forecast under different grid applications. J Energy Storage 2020 Jun 1;29:101391.
[36] Baure G, Devie A, Dubarry M. Battery durability and reliability under electric utility grid operations: path dependence of battery degradation. J Electrochem Soc 2019 Jun 12;166(10):A1991.
[37] Dubarry M, Devie A. Battery durability and reliability under electric utility grid operations: representative usage aging and calendar aging. J Energy Storage 2018 Aug 1;18:185–95.
[38] Xiong R, Pan Y, Shen W, Li H, Sun F. Lithium-ion battery aging mechanisms and diagnosis method for automotive applications: recent advances and perspectives. Renew Sustain Energy Rev 2020 Oct 1;131:110048.
[39] Gao Y, Jiang J, Zhang C, Zhang W, Ma Z, Jiang Y. Lithium-ion battery aging mechanisms and life model under different charging stresses. J Power Sources 2017 Jul 15;356:103–14.
[40] Stroe DI. Lifetime models for Lithium-ion batteries used in virtual power plant applications. Aalborg, Denmark: Dept. of Energy Tech., Aalborg University; 2014. Ph.D. dissertation.
[41] Wei M, Balaya P, Ye M, Song Z. Remaining useful life prediction for 18650 sodium-ion batteries based on incremental capacity analysis. Energy 2022 Dec 15;261:125151.
[42] Zhang H, Wang F, Xu B, Fiebig W. Extending battery lifetime for electric wheel loaders with electric-hydraulic hybrid powertrain. Energy 2022 Dec 15;261:125190.
[43] Barré A, Deguilhem B, Grolleau S, Gérard M, Suard F, Riu D. A review on lithium-ion battery ageing mechanisms and estimations for automotive applications. J Power Sources 2013 Nov 1;241:680–9.
[44] Thomas EV, Bloom I, Christophersen JP, Battaglia VS. Rate-based degradation modeling of lithium-ion cells. J Power Sources 2012 May 15;206:378–82.
[45] Delacourt C, Safari M. Life simulation of a graphite/LiFePO4 cell under cycling and storage. J Electrochem Soc 2012 Jul 20;159(8):A1283.
[46] Grolleau S, Delaille A, Gualous H, Gyan P, Revel R, Bernard J, Redondo-Iglesias E, Peter J, Network SI. Calendar aging of commercial graphite/LiFePO4 cell–Predicting capacity fade under time dependent storage conditions. J Power Sources 2014 Jun 1;255:450–8.
[47] Sarasketa-Zabala E, Gandiaga I, Rodriguez-Martinez LM, Villarreal I. Calendar ageing analysis of a LiFePO4/graphite cell with dynamic model validations: towards realistic lifetime predictions. J Power Sources 2014 Dec 25;272:45–57.
[48] Swierczynski M, Stroe DI, Stan AI, Teodorescu R, Kær SK. Lifetime estimation of the nanophosphate $\hbox {LiFePO} _ {4}\hbox {/C} $ battery chemistry used in fully electric vehicles. IEEE Trans Ind Appl 2015 Feb 19;51(4):3453–61.
[49] Ekström H, Lindbergh G. A model for predicting capacity fade due to SEI formation in a commercial graphite/LiFePO4 cell. J Electrochem Soc 2015 Mar 10;162(6):A1003.
[50] Petit M, Prada E, Sauvant-Moynot V. Development of an empirical aging model for Li-ion batteries and application to assess the impact of Vehicle-to-Grid strategies on battery lifetime. Appl Energy 2016 Jun 15;172:398–407.
[51] Sarasketa-Zabala E, Gandiaga I, Martinez-Laserna E, Rodriguez-Martinez LM, Villarreal I. Cycle ageing analysis of a LiFePO4/graphite cell with dynamic model validations: towards realistic lifetime predictions. J Power Sources 2015 Feb 1;275:573–87.
[52] Wang J, Liu P, Hicks-Garner J, Sherman E, Soukiazian S, Verbrugge M, Tataria H, Musser J, Finamore P. Cycle-life model for graphite-LiFePO4 cells. J Power Sources 2011 Apr 15;196(8):3942–8.
[53] Gering KL. Novel method for evaluation and prediction of capacity loss metrics in li-ion electrochemical cells. Electrochim Acta 2017 Feb 20;228:636–51.
[54] Bradbury K, Pratson L, Patiño-Echeverri D. Economic viability of energy storage systems based on price arbitrage potential in real-time US electricity markets. Appl Energy 2014 Feb 1;114:512–9.
[55] Shabani M, Dahlquist E, Wallin F, Yan J. Techno-economic comparison of optimal design of renewable-battery storage and renewable micro pumped hydro storage power supply systems: a case study in Sweden. Appl Energy 2020 Dec 1;279:115830.
[56] Truong CN, Naumann M, Karl RC, Müller M, Jossen A, Hesse HC. Economics of residential photovoltaic battery systems in Germany: the case of Tesla's Powerwall. Batteries 2016 Jun;2(2):14.
[57] Shabani M, Dahlquist E, Wallin F, Yan J. Techno-economic impacts of battery performance models and control strategies on optimal design of a grid-connected PV system. Energy Convers Manag 2021 Oct 1;245:114617.
[58] Mayer MJ, Szilágyi A, Gróf G. Environmental and economic multi-objective optimization of a household level hybrid renewable energy system by genetic algorithm. Appl Energy 2020 Jul 1;269:115058.
[59] He Y, Guo S, Zhou J, Wu F, Huang J, Pei H. The quantitative techno-economic comparisons and multi-objective capacity optimization of wind-photovoltaic hybrid power system considering different energy storage technologies. Energy Convers Manag 2021 Feb 1;229:113779.
[60] Shabani M, Dahlquist E, Wallin F, Yan J. Comparison of the optimal design of PV-battery and PV-PHS off-grid energy systems-a case study in Sweden. In: The 11th International Conference of Applied Energy (ICAE). Västerås, Sweden: Mälardalen University; Aug 2019.
[61] Li J. Optimal sizing of grid-connected photovoltaic battery systems for residential houses in Australia. Renew Energy 2019 Jun 1;136:1245–54.
[62] Ashtiani MN, Toopshekan A, Astaraei FR, Yousefi H, Maleki A. Techno-economic analysis of a grid-connected PV/battery system using the teaching-learning-based optimization algorithm. Sol Energy 2020 Jun 1;203:69–82.
[63] Anoune K, Ghazi M, Bouya M, Laknizi A, Ghazouani M, Abdellah AB, Astito A. Optimization and techno-economic analysis of photovoltaic-wind-battery based hybrid system. J Energy Storage 2020 Dec 1;32:101878.
[64] Telaretti E, Ippolito M, Dusonchet L. A simple operating strategy of small-scale battery energy storages for energy arbitrage under dynamic pricing tariffs. Energies 2015 Dec 25;9(1):12.
[65] Zhang Y, Ma T, Campana PE, Yamaguchi Y, Dai Y. A techno-economic sizing method for grid-connected household photovoltaic battery systems. Appl Energy 2020 Jul 1;269:115106.
[66] Zhang Y, Campana PE, Lundblad A, Yan J. Comparative study of hydrogen storage and battery storage in grid connected photovoltaic system: storage sizing and rule-based operation. Appl Energy 2017 Sep 1;201:397–411.
[67] Alramlawi M, Gabash A, Mohagheghi E, Li P. Optimal operation of hybrid PV-battery system considering grid scheduled blackouts and battery lifetime. Sol Energy 2018 Feb 1;161:125–37.
[68] García-Triviño P, Fernández-Ramírez LM, Gil-Mena AJ, Llorens-Iborra F, García-Vázquez CA, Jurado F. Optimized operation combining costs, efficiency and lifetime of a hybrid renewable energy system with energy storage by battery and hydrogen in grid-connected applications. Int J Hydrogen Energy 2016 Dec 28;41(48):23132–44.
[69] Zhang Y, Lundblad A, Campana PE, Benavente F, Yan J. Battery sizing and rule-based operation of grid-connected photovoltaic-battery system: a case study in Sweden. Energy Convers Manag 2017 Feb 1;133:249–63.
[70] Fares RL, Webber ME. What are the tradeoffs between battery energy storage cycle life and calendar life in the energy arbitrage application? J Energy Storage 2018 Apr 1;16:37–45.
[71] Liu J, Wang M, Peng J, Chen X, Cao S, Yang H. Techno-economic design optimization of hybrid renewable energy applications for high-rise residential buildings. Energy Convers Manag 2020 Jun 1;213:112868.
[72] Hesse HC, Martins R, Musilek P, Naumann M, Truong CN, Jossen A. Economic optimization of component sizing for residential battery storage systems. Energies 2017 Jul;10(7):835.
[73] Mulleriyawage UG, Shen WX. Optimally sizing of battery energy storage capacity by operational optimization of residential PV-Battery systems: an Australian household case study. Renew Energy 2020 Nov 1;160:852–64.
[74] Narayan N, Papakosta T, Vega-Garita V, Qin Z, Popovic-Gerber J, Bauer P, Zeman M. Estimating battery lifetimes in Solar Home System design using a practical modelling methodology. Appl Energy 2018 Oct 15;228:1629–39.
[75] Lindahl J. National survey report of PV power applications in Sweden. 2020. https://iea-pvps.org/.
[76] Nord Pool Spot. https://www.nordpoolgroup.com/. [Accessed 1 July 2022]. accessed.
[77] Lazard's levelized cost of storage analysis—version 5.0. 2019.
[78] Hinz H. Comparison of Lithium-Ion battery models for simulating storage systems in distributed power generation. Inventions 2019 Sep;4(3):41.
[79] Zhang S, Tang Y. Optimal schedule of grid-connected residential PV generation systems with battery storages under time-of-use and step tariffs. J Energy Storage 2019 Jun 1;23:175–82.
[80] Sweden Discount rate. 2022. Available at: http://www.riksbank.se/. [Accessed 5 June 2022]. accessed.
[81] Shabani M, Mahmoudimehr J. Influence of climatological data records on design of a standalone hybrid PV-hydroelectric power system. Renew Energy 2019 Oct 1;141:181–94.